

## Rapid report

# A cell surface arabinogalactan-peptide influences root hair cell fate

Author for correspondence:


José M. Estevez

Tel: +54 115 238 7500, ext. 3206

Email: [jestevez@leloir.org.ar](mailto:jestevez@leloir.org.ar)

Received: 4 December 2019

Accepted: 12 February 2020

**Cecilia Borassi<sup>1\*</sup>, Javier Gloazzo Dorosz<sup>1\*</sup>, Martiniano M. Ricardi<sup>2\*</sup>, Mariana Carignani Sardoy<sup>1</sup>, Laercio Pol Fachin<sup>3</sup>, Eliana Marzol<sup>1</sup>, Silvina Mangano<sup>1</sup>, Diana Rosa Rodríguez García<sup>1</sup>, Javier Martínez Pacheco<sup>1</sup>, Yossmayer del Carmen Rondón Guerrero<sup>1</sup>, Silvia M. Velasquez<sup>1</sup>, Bianca Villavicencio<sup>4</sup>, Marina Ciancia<sup>5,6</sup>, Georg Seifert<sup>7</sup>, Hugo Verli<sup>4</sup> and José M. Estevez<sup>1,8,9</sup> **

<sup>1</sup>Fundación Instituto Leloir and IIBBA-CONICET, Av. Patricias Argentinas 435, Buenos Aires, Argentina; <sup>2</sup>Departamento de Fisiología y Biología Molecular y Celular (FBMC), Facultad de Ciencias Exactas y Naturales, Instituto de Fisiología, Biología Molecular y Neurociencias (IFByNE-CONICET), Universidad de Buenos Aires, CP C1405BWE, Buenos Aires C1428EGA, Argentina; <sup>3</sup>Centro Universitario CESMAC, Maceió 57051160, Brazil; <sup>4</sup>Centro de Biotecnología, Universidade Federal do Rio Grande do Sul, CP 15005, Porto Alegre 91500-970 RS, Brazil; <sup>5</sup>Departamento de Biología Aplicada y Alimentos, Facultad de Agronomía, Cátedra de Química de Biomoléculas, Universidad de Buenos Aires, Buenos Aires, Argentina; <sup>6</sup>Centro de Investigación de Hidratos de Carbono (CIHIDECAR), CONICET-Universidad de Buenos Aires, C1428EGA, Buenos Aires, Argentina; <sup>7</sup>Department of Applied Genetics and Cell Biology, University of Natural Resources and Life Science, BOKU Vienna, Muthgasse 11, A-1190, Vienna, Austria; <sup>8</sup>Centro de Biotecnología Vegetal (CBV), Facultad de Ciencias de la Vida, Universidad Andrés Bello, Santiago 8370186, Chile; <sup>9</sup>Millennium Institute for Integrative Biology (iBio), Santiago 8331150, Chile

### Summary

- Root hairs (RHs) develop from specialized epidermal trichoblast cells, whereas epidermal cells that lack RHs are known as atrichoblasts. The mechanism controlling RH cell fate is only partially understood.
- RH cell fate is regulated by a transcription factor complex that promotes the expression of the homeodomain protein GLABRA 2 (GL2), which blocks RH development by inhibiting ROOT HAIR DEFECTIVE 6 (RHD6). Suppression of GL2 expression activates RHD6, a series of downstream TFs including ROOT HAIR DEFECTIVE 6 LIKE-4 (RSL4) and their target genes, and causes epidermal cells to develop into RHs. Brassinosteroids (BRs) influence RH cell fate. In the absence of BRs, phosphorylated BIN2 (a Type-II GSK3-like kinase) inhibits a protein complex that regulates GL2 expression.
- Perturbation of the arabinogalactan peptide (AGP21) in *Arabidopsis thaliana* triggers aberrant RH development, similar to that observed in plants with defective BR signaling. We reveal that an O-glycosylated AGP21 peptide, which is positively regulated by BZR1, a transcription factor activated by BR signaling, affects RH cell fate by altering GL2 expression in a BIN2-dependent manner.
- Changes in cell surface AGP disrupts BR responses and inhibits the downstream effect of BIN2 on the RH repressor GL2 in root epidermis.

*New Phytologist* (2020) **227**: 732–743  
doi: 10.1111/nph.16487

**Key words:** *Arabidopsis thaliana*, arabinogalactan peptide 21, brassinosteroids, O-glycosylation, root hair cell fate.

### Introduction

Plant roots not only anchor the plant into the soil but also allow them to absorb water and nutrients from the soil. Root hairs (RHs)

are single cell protrusions developed from the epidermis that increase the root surface area exposed to the soil enhancing water and nutrients uptake. Many factors determine whether, or not, an epidermal cell will develop into a RH. These factors include both, environmental cues (such as nutrients in the soil) and signals from the plant itself, such as hormones like brassinosteroids (BRs), ABA,

\*These authors contributed equally to this work.

ethylene and auxin (Masucci & Schiefelbein, 1994, 1996; Van Hengel *et al.*, 2004; Kuppusamy *et al.*, 2009). RH cell fate in the model plant *Arabidopsis* is controlled by a well-known developmental program, regulated by a complex of transcription factors composed by WEREWOLF (WER)-GLABRA3 (GL3)/ENHANCER OF GLABRA3 (EGL3)-TRANSPARENT GLABRA1 (TTG1) that promotes the expression of the homeodomain protein GLABRA 2 (GL2) (Ryu *et al.*, 2005; Song *et al.*, 2011; Schiefelbein *et al.*, 2014; Balcerowicz *et al.*, 2015), which ultimately blocks the RH pathway by inhibiting ROOT HAIR DEFECTIVE 6 (RHD6) (Lin *et al.*, 2015). The suppression of GL2 expression triggers epidermal cells to enter into the RH cell fate program by the concomitant activation of RHD6 and a well-defined downstream gene network. As a consequence, RH and non-RH cell files are patterned alternately in rows within the root epidermis. In trichoblasts, a second transcription factor complex composed by CAPRICE (CPC)-GL3/EGL3-TTG1 suppresses GL2 expression (Schiefelbein *et al.*, 2014), forcing cells to enter the RH cell fate program via concomitant RHD6 activation and downstream TFs, including RSL4, and RH genes (Yi *et al.*, 2010). The plant steroid hormones, BRs play essential roles in regulating many developmental processes (Savaldi-Goldstein *et al.*, 2007; Hacham *et al.*, 2011; Yang *et al.*, 2011). BRs are perceived by the receptor kinase BRASSINOSTEROID INSENSITIVE 1 (BRI1) (Li & Chory, 1997; Hothorn *et al.*, 2011; She *et al.*, 2011). One of the BRI1 substrate, BR-SIGNALING KINASE (BSK), transduces the BR signaling through *bri1* SUPPRESSOR 1 (BSU1) to inactivate a GSK3-like kinase BRASSINOSTEROID INSENSITIVE 2 (BIN2), which triggers high levels of the dephosphorylated form of transcriptional factors BRI1 EMS SUPPRESSOR 1 (BES1)/BRASSINAZOLE RESISTANT 1 (BZR1) in the nucleus to regulate gene expression (Yan *et al.*, 2009; Yang *et al.*, 2011). In recent years, a molecular mechanism was proposed by which BR signaling controls RH cell fate by inhibiting BIN2 phosphorylation activity to positively modulate *GL2* expression thus hindering the RH development in trichoblast cells and promoting the lack of RHs in the root epidermis (Cheng *et al.*, 2014). On the contrary, phosphorylated BIN2 under the absence/low amounts of BRs, is able to phosphorylate TTG1, controlling protein complex TTG1-WER-GL3/EGL3 activity and repressing *GL2* expression to promote anomalous RH development in atrichoblast cells (Cheng *et al.*, 2014). The later scenario produces contiguous RH in the root epidermis that is unusual in Wt Col-0 roots.

Plant cell surface proteoglycans known as arabinogalactan proteins (AGPs) function in a broad developmental processes such as cell proliferation, cell expansion, organ extension, and somatic embryogenesis (Tan *et al.*, 2004; Seifert & Roberts, 2007; Pereira *et al.*, 2015; Ma *et al.*, 2018). The precise mechanisms underlying AGP action in these multiple processes are completely unknown (Ma *et al.*, 2018). AGP peptides are post-translationally modified in the ER-Golgi, undergoing signal peptide (SP) removal, proline-hydroxylation/Hyp-*O*-glycosylation, and C-terminal GPI anchor signal (GPI-AS) addition (Schultz *et al.*, 2004; Ma *et al.*, 2018). Processed mature AGP-peptides are 10–13 amino acids long and bear few putative *O*-glycosylation sites (*O*-AG). Few prolines in the

AGP peptides are hydroxylated *in vivo* as Hyp (Hyp=O), suggesting that AGP peptides are *O*-glycosylated at maturity (Schultz *et al.*, 2004). All these posttranslational modifications make the study of AGPs very complex with almost no defined biological functions for any individual AGP (Ma *et al.*, 2018). Interestingly, in this work we have identified that disruption of plant specific AGPs, and in particular of a single *O*-glycosylated AGP peptide (AGP21), interfere in a specific manner with BR responses and BIN2-downstream effect on the repression of RH development. We have found that the absence of an *O*-glycosylated AGP21-peptide, positively regulated by the BR transcription factor BZR1, impacts on RH cell fate in a BIN2-dependent manner by controlling in a negative manner the *GL2* expression and enhancing the expression of the downstream RH specific genes *RHD6*, *RSL4* and *EXP7*.

## Materials and Methods

### Growth conditions

All plant materials used in this study were in the Columbia-0 ecotype background of *Arabidopsis thaliana*. Seeds were sterilized and placed on half-strength (½MS) Murashige and Skoog (MS) medium (Sigma-Aldrich) pH 5.8 supplemented with 0.8% agar. For root measurements, RNA extraction and confocal microscopy 7-d old seedlings were grown on square plates placed vertically at 22°C with continuous light, after stratification in dark at 4°C for 5 d on the plates. Seedlings on plates were transferred to soil and kept in the glasshouse in long-day conditions to obtain mature plants for transformation, genetic crossing, and amplification of seeds.

### Plant material

For identification of homozygous T-DNA knockout lines, genomic DNA was extracted from rosette leaves. Confirmation by PCR of a unique band corresponding to T-DNA insertion in the target genes AGP15 (At5G11740: SALK\_114736), AGP21 (At1G55330: SALK\_140206), HPGT1-HPGT3 (AT5G53340: SALK\_007547, AT4G32120: SALK\_070368, AT2G25300: SALK\_009405) GALT29A (At1G08280: SALK\_030326; SALK\_113255; SAIL\_1259\_C01) and RAY1 (At1G70630: SALK\_053158) were performed using an insertion-specific LBb1.3 for SALK lines or Lb1 for SAIL lines. Primers used are listed in Supporting Information Table S1. The stable transgenic lines used in this study are summarized in Table S2.

### Pharmacological treatments

Ethyl-3,4-dihydroxybenzoate (EDHB) and  $\alpha,\alpha$ -bipyridyl (DP, D216305; Sigma-Aldrich) were used as P4Hs inhibitors. DP chelates the cofactor Fe<sup>2+</sup> [9] and the EDHB interacts with the oxoglutarate-binding site of P4Hs (Majamaa *et al.*, 1986). Specific Yariv phenylglycoside (for 1,3,5-tri-(*p*-glycosyloxyphenylazo)-2,4,6-trihydroxybenzene),  $\beta$ -glucosyl Yariv phenylglycoside ( $\beta$ -Glc-Y) was used for AGP-depletion (Kitazawa *et al.*, 2013).

$\alpha$ -Mannosyl Yariv phenylglycoside ( $\alpha$ -Man-Y) was used as negative control for phenylglycoside treatment. Both,  $\beta$ -Glc-Y and  $\alpha$ -Man-Y are Yariv-phenylglycosides and its specificity for AGPs relies on the  $\beta$ -configuration of the glycosyl residues attached to the phenylazotrihydroxybenzene core (Yariv *et al.*, 1967). DP, EDHB, or Yariv reagents were added to MS media when MS plates were made. Seedlings were grown for 4 d in  $\frac{1}{2}$ MS media and then transferred for 3 d more to  $\frac{1}{2}$ MS plates with DP, EDHB or Yariv reagents at the concentration indicated.

### Quantification of RH cell fate

In order to determine the RH patterning, images of root tips were taken using an Olympus stereomicroscope at maximum magnification ( $\times 50$ ). The presence of contiguous RH was analyzed using IMAGEJ, starting from the differentiation zone to the elongation zone. The amount of contiguous RH was expressed as a percentage of total RH for rectangular root areas of 200  $\mu\text{m}$  in width  $\times$  2 mm in length ( $n = 20$ ) with three biological replicates. Quantitative and statistical analysis was carried on using GRAPHPAD software. To analyze the alteration in RH cell fate, root cell walls of reporter lines were stained with  $5 \mu\text{g ml}^{-1}$  propidium iodide and confocal microscopy images were taken using a Zeiss LSM 710 Pascal microscope,  $\times 40$  objective  $N/A = 1.2$ .

### RH density measurements

RH density was determined as the number of RHs in  $1 \text{ mm}^2$  segments of root epidermis from 7 d old seedlings. Images of roots were taken using an Olympus stereomicroscope at maximum magnification ( $\times 50$ ). At least six plants were measured for each genotype, and each experiment was replicated three times. Correlation analysis was performed to determine the relationship between the percentage of contiguous RH % and RH density per genotype.

### AGP21 variants

AGP21 promoter region (AGP21p) comprising 1.5 kbp upstream of +1 site was amplified by PCR and cloned into pGWB4 to obtain AGP21p::GFP construct. Synthetic DNA was designed containing full length AGP21 cDNA and Venus fluorescent protein cDNA between AGP21 signal sequence and the mature polypeptide (Venus-AGP21), containing Gateway™ (Life Technologies, Carlsbad, CA, USA) attB1 and attB2 sites. Recombinase-mediated integration of the PCR fragment was made into pEntry4Dual. pEntry4Dual/Venus-AGP21 construction was recombined into the vector pGWB2 (Hygromycin R, Invitrogen, Carlsbad, CA, USA) in order to overexpress Venus-AGP21 under 35S mosaic virus promoter (35S::Venus-AGP21). Also, Venus-AGP21 construct was cloned into pGWB1 (no promoter, no tag) and AGP21p was sub-cloned in the resulting vector to express AGP21 reporter under the control of its endogenous promoter (AGP21::Venus-AGP21). Wild-type and T-DNA *agp21* mutant plants were transformed by using *Agrobacterium* (strain GV3101+pSoup). Plants were selected with hygromycin ( $30 \mu\text{g ml}^{-1}$ ) and several

independent transgenic plants were isolated for each construct. At least three homozygous independent transgenic lines of Col-0/AGP21::GFP, *agp21*/AGP21::Venus-AGP21 and *agp21*/35S::AGP21-GFP were obtained and characterized.

### Gene expression analysis

For reverse transcription polymerase chain reaction (RT-PCR) analysis, total RNA was isolated from roots of 7-d-old seedlings using RNeasy Plant Mini Kit (Qiagen, Hilden, Germany) according to the manufacturer's instructions. cDNA synthesis was achieved using M-MLV reverse transcriptase (Promega, Madison, WI, USA). PCR reactions were performed in a T-Advanced S96G (Biometra, Jena, Germany) using the following amplification program: 4 min at  $95^\circ\text{C}$ , followed by 35 cycles of 20 s at  $95^\circ\text{C}$ , 30 s at  $57^\circ\text{C}$  and 30 s at  $72^\circ\text{C}$ . RT-PCR was performed to assess AGP15 and AGP21 transcript levels in wild-type and T-DNA mutant *agp15* and *agp21*. PP2A was used as an internal standard. All primers used are listed in Table S1.

### Confocal microscopy

Confocal laser scanning microscopy was performed using Zeiss LSM 510 Meta and Zeiss LSM 710 Pascal (Oberkochen, Germany). Fluorescence was analyzed by using laser lines of 488 nm for GFP or 514 nm for YFP excitation, and emitted fluorescence was recorded between 490 and 525 nm for GFP and between 530 and 600 nm for YFP ( $\times 40$  objective,  $N/A = 1.2$ ). Z series was done with an optical slice of  $1 \mu\text{m}$ . Fluorescence intensities were summed for quantification along a segmented line comprising both in trichoblast and atrichoblast cell layers (starting at the meristematic zone towards the differentiation zone). For the quantification of fluorescence corresponding to Venus-AGP21 in control roots and roots treated with  $\beta$ -Glc-Y or with BL, the plot profile command in IMAGEJ was used, five replicates for each root ( $n = 5$ ) were observed. Statistical analysis was performed using GRAPHPAD (v.5). In a similar manner, to quantify the levels of expression of *AGP21::V-AGP21* in trichoblast and atrichoblast cell layers in the root meristematic zone, a plot profile line of  $100 \mu\text{m}$  in length from the root tip to the expansion zone was recorded in IMAGE J and five replicates for each root ( $n = 5$ ) were observed.

### AGP21 immunoblotting detection

Proteins were extracted from roots of 7-d-old seedlings using extraction buffer (20 mM Tris-HCl pH 8.8, 150 mM NaCl, 1 mM EDTA, 20% glycerol, 1 mM PMSF,  $1\times$  protease inhibitor Complete® Roche, Basel, Switzerland) at  $4^\circ\text{C}$ . After centrifugation at  $21\,000 \text{ g}$  at  $4^\circ\text{C}$  for 20 min, protein concentration in the supernatant was measured and equal protein amounts were loaded onto a 6% sodium dodecyl sulfate–polyacrylamide gel electrophoresis (SDS-PAGE) gel. Proteins were separated by electrophoresis and transferred to nitrocellulose membranes. Anti-GFP mouse IgG (Roche Applied Science, Penzberg, Germany) was used at a dilution of 1 : 1000 and it was visualized by incubation with goat anti-mouse IgG secondary antibodies conjugated to horseradish

peroxidase (1 : 10 000) followed by a chemiluminescence reaction (Clarity™ Western ECL Substrate; Bio-Rad, Hercules, CA, USA).

### Transient expression assays in *Nicotiana benthamiana*

To test the sub-cellular localization of AGP21, 5-d-old *Nicotiana benthamiana* leaves were infiltrated with *Agrobacterium* strains (GV3101) carrying 35S::Venus-AGP21 and BAK1-RFP constructs. After 2 d, images of the lower leaf epidermal cells were taken using a confocal microscope (LSM5 Pascal, Zeiss, Jena, Germany) to analyze Venus-AGP21 expression. Plasmolysis was done using 800 mM mannitol.

### Molecular dynamic (MD) simulations

Molecular dynamic (MD) simulations were performed on two nonglycosylated and seven glycosylated Ala1-Pro2-Ala3-Pro4-Ser5-Pro6-Thr7-Ser8 (APAPSPTS) peptides, in which the starting structure was constructed as a type-II polyproline helix, with  $\varphi \approx -75$  and  $\psi \approx 145$ . The nonglycosylated motifs differ by the presence of alanine (AAAASATS), proline (APAPSPTS) or 4-*trans*-hydroxyproline (AOAOSOTS) residues. At the same time, the glycosylated motifs reflect different peptideglycoforms, constructed as full glycosylated (AOAOSOTS). Every *O*-glycosylation site was filled with an arabinogalactan oligosaccharide moiety (Fig. S6b), in which the *O*-glycan chains and carbohydrate-amino acid connections were constructed based on the most prevalent geometries obtained from solution MD simulations of their respective disaccharides, as previously described (Pol-Fachin & Verli, 2012), thus generating the initial coordinates for glycopeptide MD calculations. Such structures were then solvated in rectangular boxes using periodic boundary conditions and the SPC water model (Berendsen *et al.*, 1984). Both carbohydrate and peptide moieties were described under GROMOS96 43a1 force field parameters, and all MD simulations and analyzes were performed with GROMACS simulation suite, v.4.5.4 (Hess *et al.*, 2008). The Lincs method (Hess *et al.*, 1997) was applied to constrain covalent bond lengths, allowing an integration step of 2 fs after an initial energy minimization using the Steepest Descents algorithm. Electrostatic interactions were calculated with the generalized reaction-field method Tironi *et al.* (1995). Temperature and pressure were kept constant at 310 K and 1.0 atom, respectively, by coupling (glyco)peptides and solvent to external baths under V-rescale thermostat Bussi *et al.*, 2007) and Berendsen barostat (Berendsen *et al.*, 1987) with coupling constants of  $t = 0.1$  and  $t = 0.5$ , respectively, via isotropic coordinate scaling. The systems were heated slowly from 50 to 310 K, in steps of 5 ps, each one increasing the reference temperature by 50 K. After this thermalization, all simulations were further extended to 100 ns. See Table S3.

## Results and Discussion

### AGP perturbation influences RH cell fate programming

To determine whether *O*-glycosylated AGPs regulate specific RH developmental processes, we exposed roots of *Arabidopsis thaliana*

to  $\beta$ -glucosyl Yariv ( $\beta$ -Glc-Y), which specifically binds structures in the *O*-glycans of AGPs: oligosaccharides with at least 5–7 units of three-linked *O*-galactoses (Yariv *et al.*, 1967; Kitazawa *et al.*, 2013).  $\beta$ -Glc-Y-linked AGP complexes on the cell surface induce AGP aggregation and disrupt native protein distribution, triggering developmental reprogramming (Guan & Nothnagel, 2004; Sardar *et al.*, 2006).  $\alpha$ -Mannosyl Yariv ( $\alpha$ -Man-Y), an analogue that does not bind to AGPs, served as the control. While  $\alpha$ -Man-Y treatment did not affect RH cell fate ( $\approx 2$ –5% of total RHs that are contiguous in a similar range present in Wt Col-0),  $\beta$ -Glc-Y treatment increased contiguous RH development ( $\approx 30$ –35%) (Fig. S1a), suggesting that *O*-glycosylated AGPs may influence RH cell fate.

To test whether *O*-glycans on hydroxyproline-rich glycoproteins (HRGPs) alter RH cell fate, we blocked proline 4-hydroxylase enzymes (P4Hs) that catalyze proline (Pro)-hydroxylation into hydroxyl-proline units (Hyp), the subsequent step of HRGP *O*-glycosylation (Velasquez *et al.*, 2011, 2015a). Two P4H inhibitors,  $\alpha$ , $\alpha$ -dipyridyl (DP) and ethyl-3,4-dihydroxybenzoate (EDHB), prevent Pro-hydroxylation (Barnett, 1970; Majamaa *et al.*, 1986); both increased contiguous RH development to  $\approx 15$ –20% (Fig. S1b). Additionally, *p4h5* (a key P4H in roots (Velasquez *et al.*, 2011, 2015a)) and four glycosyltransferase (GT) mutants defective in AGP and related proteins *O*-glycosylation (*hpgt* triple mutant; *ray1*, *galt29A*, and *fut4 fut6*) (see Table S4) showed significantly increased ( $\approx 8$ –20%) ectopic RH development (Fig. 1a), sustaining the previous report that the triple mutant *hpgt* mutant has an increased RH density (Ogawa-Ohnishi & Matsubayashi, 2015). These mutants were mostly insensitive to  $\beta$ -Glc-Y; however, the treatment increased the number of contiguous RHs in *fut4 fut6*, although to a lesser extent than in the wild-type (Fig. 1b). This minor effect is expected since *O*-fucosylation in AGPs occurs at low levels in roots (Tryfona *et al.*, 2014).  $\beta$ -Glc-Y inhibits root cell expansion (Willats & Knox, 1996; Ding & Zhu, 1997). On the contrary, glycosyltransferase (GT) mutations affecting extensin (EXTs) and related proteins *O*-glycosylation (e.g. *rra3* and *sgt1 rra3*; Table S4) drastically affect only RH cell elongation (Velasquez *et al.*, 2015b). These mutations did not affect RH cell fate, and  $\beta$ -Glc-Y stimulated ectopic RH development as in Wt Col-0, indicating that EXT *O*-glycosylation might not function in RH cell fate reprogramming (Table S4; Fig. 1c), and specifically *O*-glycans attached to AGPs and related glycoproteins do. P4H5 and AGP-related GTs (e.g. RAY1, GALT29A, HPGT1-HPGT3 and FUT4/FUT6), are expressed in the root epidermis elongation and differentiation zones (Fig. S2). Under-arabinosylated AGPs in *ray1* and, to a lower extent, under-*O*-fucosylated AGPs in *fut4 fut6* show root growth inhibition (Liang *et al.*, 2013; Tryfona *et al.*, 2014), highlighting a key role for AGP *O*-glycans in regulating root growth, albeit by unknown mechanisms. Our results using DP/EDHB and  $\beta$ -Glc-Y treatments as well as mutants in the AGPs *O*-glycosylation pathway suggest that AGPs and related proteins might be involved in RH cell fate.

### The AG peptide AGP21 influences RH cell fate

Brassinosteroid (BR) signaling regulates RH cell patterning (Cheng *et al.*, 2014). The BR-insensitive mutant, *bri1-116*, and *bak1*

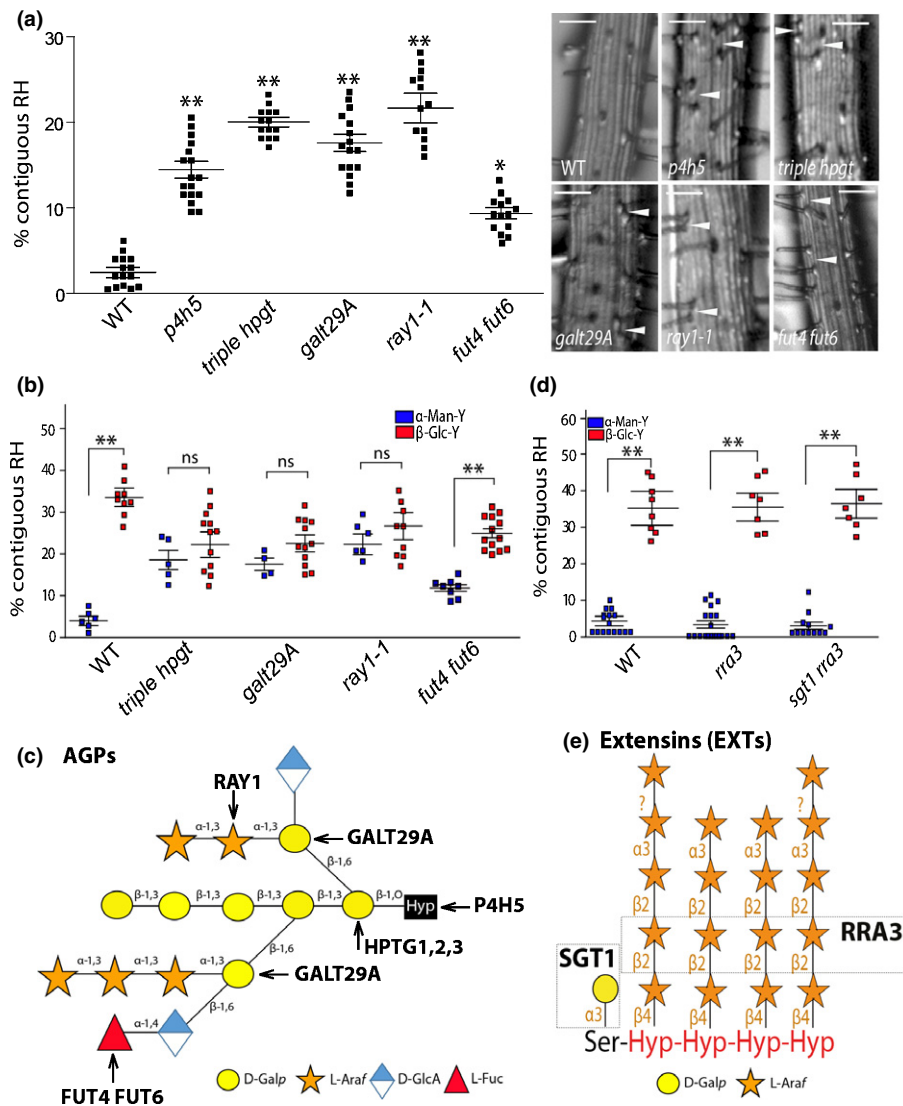


**Fig. 1** Contiguous root hair (RH) phenotype in O-underglycosylated arabinogalactan proteins (AGPs) phenocopy brassinosteroid (BR) mutants in *Arabidopsis thaliana*. (a) RH phenotype in three glycosyltransferase (GT) mutants (*triple hpgt*, *ray1*, *galt29A* and *fut4 fut6*) that act specifically on AGP O-glycosylation. Effect on contiguous RH phenotype in roots treated with 5 μM α-mannosyl Yariv (α-Man-Y) or 5 μM β-glucosyl Yariv (β-Glc-Y). (b) RH phenotype in the *p4h5* mutant and in four glycosyltransferase mutants (*triple hpgt*, *ray1*, *galt29A*, and *fut4 fut6*) that act specifically on AGP O-glycosylation. Right, selected pictures. Arrowheads indicated two contiguous RHs. Bars, 50 μm. (c) The mutants used in (b) for the GTs involved in AGP O-glycosylation are indicated. (d) RH phenotype in two glycosyltransferase mutants (*rra3* and *rra3 sgt1*) that act specifically on EXT O-glycosylation. Effect on contiguous RH phenotype in roots treated with 5 μM α-Man-Y or β-Glc-Y. (e) The mutants used in (d) for the GTs involved in EXT O-glycosylation are indicated. (a, b and d) *P*-value of one-way ANOVA: \*\*, *P* < 0.001; \*, *P* < 0.01; ns, not significant different. Error bars indicate ± SD from biological replicates. See also Supporting Information Figs S1–S4.

developed many ( $\approx 20$ –25%) contiguous RH cells (Fig. S3a), resembling plants subjected to β-Glc-Y and DP/EDHB treatments (Fig. S1). *p4h5*, *hpgt* triple mutant, *ray1-1*, *galt29A*, and *fut4 fut6* mutants exhibited similar phenotypes, suggesting that an interplay between cell surface AGPs and BR signaling may determine RH cell fate. Chromatin-immunoprecipitation (ChIP)-sequencing and RNA-sequencing indicated that BZR1 directly upregulates few AGPs gene expression, most predominantly *AGP21* (Sun *et al.*, 2010). Based on this, we decided to investigate how root epidermal BR signaling regulates *AGP21* expression. Since the *AGP21* regulatory region contains one BZR1 binding motif (E-BOX, CATGTG at –279 bp relative to ATG start codon), we tested whether BR directly modulates *AGP21* expression. Compared with no treatment, 100 nM BL (brassinolide, BR's most active form) enhanced of both *AGP21p::GFP* (transcriptional reporter) and *AGP21p::V-AGP21* (V = Venus tag; translational reporter) expression (Fig. S3b,c). Expression of *AGP21p::GFP* in *bri1-116* resulted in lower *AGP21* signal than in untreated wild-type (Fig. S3b), confirming that BR-mediated BZR1 controls *AGP21*

expression in the root. To visualize if drastic changes are induced under β-Glc-Y treatment on epidermis cells and AGPs, we decided to analyze the localization of *AGP21p::V-AGP21* in this condition. Treatment with β-Glc-Y—but not α-Man-Y—resulted in a clear accumulation of *AGP21p::Venus-AGP21* protein at transverse cell walls in the root epidermis (Fig. S1c), thus confirming the expected effect on aggregating AGPs at the cell surface by β-Glc-Y treatment. It is unclear why *AGP21* with β-Glc-Y accumulates only in the transversal walls but not all over the cell walls. These results point out *AGP21* as a possible link between RH cell fate phenotype and BR responses in root epidermal cells.

Although we screen for abnormal RH cell fate in several AGP-peptide mutants, only *AGP21* deficient mutant *agp21*, and to a lower extent, *agp15* (Fig. S4a,b), exhibited ectopic contiguous RHs at high levels ( $\approx 20\%$  and  $12\%$ , respectively; Fig. 2a). Both *AGP21* expression under its endogenous promoter (*AGP21p::V-AGP21/agp21*) and overexpression (*35Sp::V-AGP21/agp21*) restored a wild-type RH phenotype and patterning to *agp21* (Fig. 2a), confirming that deficient *AGP21* expression causes contiguous RH

development. Furthermore, while  $\beta$ -Glc-Y treatment triggered up to  $\approx 35\%$  of contiguous RH (vs  $\approx 2\text{--}5\%$  induced by  $\alpha$ -Man-Y) in the wild-type (Fig. S1a), it induced no additional anomalous RH in *agp21* (vs  $\alpha$ -Man-Y treatment or untreated roots) (Fig. 2a). We tested whether the closely related BZR1-induced peptide AGP15 functions with AGP21 (Sun *et al.*, 2010). *agp15* (Fig. S4c–d) exhibited a milder phenotype than *agp21*, and the double *agp15 agp21* double mutant had no additional effects to *agp21* (Fig. S4e). Together, these results confirm that  $\beta$ -Glc-Y might affect *O*-glycosylated AGP21 to stimulate contiguous RH development. The contiguous RH phenotype detected in all genotypes including *agp21* and Yariv-treated roots in this study positively correlates with a higher density of RH in the root epidermis in the same lines in a linear manner ( $r^2 = 0.795$ ) (Fig. S4f). This confirms that contiguous RH phenotype produces more RHs per epidermis area.

### O-Glycosylation is required for the correct targeting of the AGP21 peptide to the plasma membrane-apoplastic space

To determine whether functional AGP21 requires *O*-glycosylation, three putative *O*-glycosylation sites were mutated (Pro $\rightarrow$ Ala) (Fig. 2b) and driven by the endogenous *AGP21* promoter in *agp21* (*AGP21p::V-AGP21<sup>ALA</sup>/agp21*). Mass spectrometry had detected that all three proline units (Pro/P) within the AGP21 sequence ATVEAPAPSPTS can be hydroxylated as ATVEAOAQSOTS (Hyp=O) (Schultz *et al.*, 2004), with underlines indicating likely sites for *O*-glycosylation. Even though AGP21<sup>ALA</sup> protein was detected in root epidermal cells (Fig. S5b), AGP21<sup>ALA</sup> failed to rescue the *agp21* RH phenotype (Fig. 2a). Moreover,  $\beta$ -Glc-Y treatment did not induce anomalous RH cell fate in AGP21<sup>ALA</sup> plants. Then, we examined whether AGP21 expressed in *Nicotiana benthamiana* colocalized with the BRI1 co-receptor BAK1 (Fig. 2c). V-AGP21 partially colocalized with BAK1-mRFP protein (Fig. 2c). When epidermal cells were plasmolyzed, most AGP21 signal localized to the apoplast but some remained close to the PM (Fig. 2c). V-AGP21<sup>ALA</sup>, however, never reached the cell surface; retention in the secretory pathway could indicate that *O*-glycans direct AGPs to the PM–cell surface (Fig. S5a,b). These data is in agreement with previous reports of a requirement for *O*-glycans in the secretion and targeting of AGPs and related fasciclin-like AGPs (Xu *et al.*, 2008; Xue *et al.*, 2017). It is important to note that when AGP21 is transiently overexpressed in *Nicotiana benthamiana*, most of the expression remains in the apoplast and AGP21 is possibly highly *O*-glycosylated (Fig. 2c,e) while the expression is under the control of its endogenous promoter in *Arabidopsis* most of the signal is linked to the plasma membrane and secretory pathway with less putative *O*-glycosylated isoforms (Figs 2d,e, S1c, S5a). This difference may be linked to both, expression and *O*-glycosylation levels of AGP21. Then, we quantify the expression levels of *AGP21p::V-AGP21* in trichoblast and atrichoblast cell layers in the root meristematic zone. Although the pattern of AGP21 expression is patchy and irregular, the overall levels of AGP21 are significantly higher in atrichoblast cell layers ( $807 \pm 87$  arbitrary units) than in trichoblast cells ( $607 \pm 31$  arbitrary units) (Fig. 2d). This is in agreement with the contiguous

RH phenotype shown by the *agp21* mutant suggesting that AGP21 function is related to atrichoblast cell fate.

We tested the hypothesis that AGP21 is processed and modified during its synthesis along the secretory pathway. Using immunoblot analysis, we examined the apparent molecular weight of AGP21 peptide in transient AGP21-overexpressing plants and in *AGP21p::V-AGP21* plants (Fig. 2e). In the overexpressing plants, most AGP21 peptide was detected as a strong broad band around  $\approx 100\text{--}120$  kDa with minor bands at  $\approx 80$  and  $\approx 55$  kDa, whereas endogenously driven AGP21 produced a stronger band at  $\approx 80$  kDa and lacked the band at  $\approx 55$  kDa, suggesting that, in both cases, AGP21 peptide might be present in a putative tri-*O*-glycosylated form. Mature peptide with no posttranslational modifications is approximately 30 kDa; the extra bands could be interpreted as intermediate single- and di-*O*-glycosylated forms of AGP21 peptide. An apparent molecular shift of  $\approx 25\text{--}30$  kDa for each putative *O*-glycosylation site in AGP21 accords with AGP14 peptide, whose protein sequence is highly similar (Ogawa-Ohnishi & Matsubayashi, 2015), and with the electrophoretic migration of an AGP-xyligen molecule that contains two arabinogalactan-*O*-Hyp sites (Motosue *et al.*, 2004). V-AGP21<sup>ALA</sup>, which lacks *O*-glycans, showed much lower expression, is not targeted to the cell surface, formed puncta-structures (Fig. S5b) and showed one band close to  $\approx 55$  kDa (Fig. 2e) and one band close to  $\approx 30$  kDa. It is hypothesized here that lack of *O*-glycans in V-AGP21<sup>ALA</sup> may cause self-interactions and this is compatible with the punctuated structure visualized in the root epidermal cells (Fig. S5b). A detailed analysis is required to characterize *O*-glycosylation in AGP21 peptide although it is technically challenging due to its carbohydrate complexity. AGP21<sup>ALA</sup> failure to rescue the *agp21* RH mutant phenotype is possibly due to several reasons, including the lack of Hyp-linked *O*-glycans on its peptide that may affect its function, its lower expression level when compared to *AGP21p::V-AGP21* (Fig. 2d), and the final cell targeting of the mutated version of AGP21 that differs from the *AGP21p::V-AGP21* functional version (Fig. S5a,b).

### O-Glycans stabilize AGP21 peptide's functional conformation

To address the effect of *O*-glycan on the conformation and stability of AGP21 peptide, we modeled a minimal, 15-sugar Hyp-*O*-linked arabinogalactan (AG) structure ([ATVEAP(O)AP(O)SP(O)TS], Fig. S6a,b). This is the simplest carbohydrate structure characterized for a single AGP synthetic peptide (Tan *et al.*, 2004), although more complex structures were described for several AGPs (Kitazawa *et al.*, 2013). To assess the conformation of AGP21 peptide and the effect of *O*-glycosylation, MD simulations considered three non-glycosylated peptides (with alanines [nG-Ala], prolines [nG-Pro], or hydroxyprolines residues [nG-Hyp], respectively) and one *O*-glycosylated peptide with three Hyp-*O*-glycans (Fig. S6c). In the MD simulations, the root mean square deviation (RMSD) varied up to  $\approx 6$  Å (Fig. S6d), indicating that peptide structure may have deviated from the starting type-II polyproline helix. By contrast, larger conformational stabilization effects were observed in the *O*-glycosylated peptide (Fig. S6e).

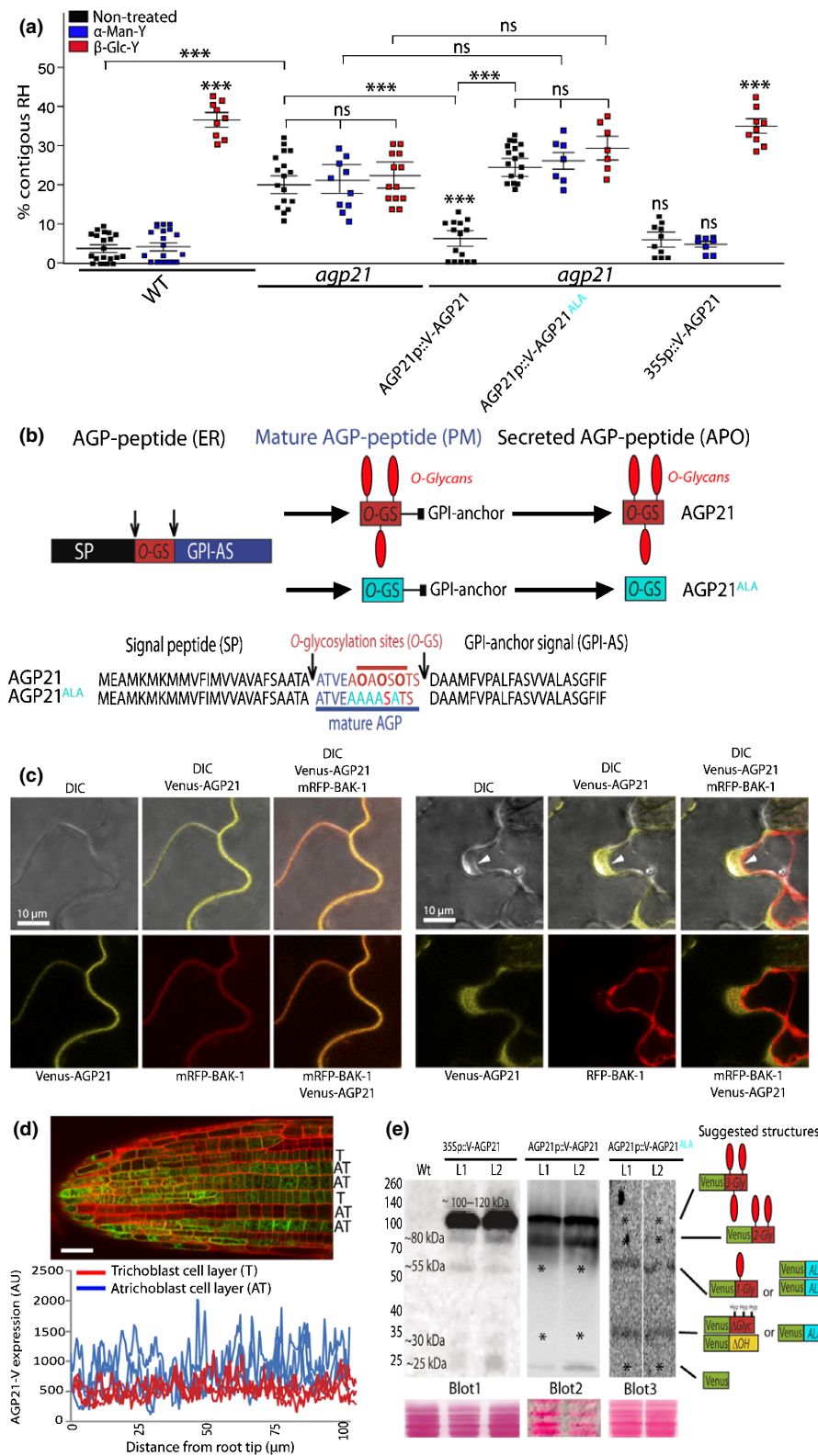


**Fig. 2** O-Glycosylated AGP21 peptide at the cell surface modulates root hair (RH) cell fate in *Arabidopsis thaliana*. (a) Contiguous RH phenotype in *agp21*, complemented *agp21* mutant with AGP21::V-AGP21 and with 35S::V-AGP21 constructs as well as AGP21::V-AGP21<sup>ALA</sup> expression in *agp21*. Only one line is shown. *P*-Value of one-way ANOVA: \*\*\*, *P* < 0.001; ns, not significant differences. Error bars indicate  $\pm$  SD from biological replicates. (b) Identified AGP21 peptide acting on root epidermis development. AGP21 peptide sequence and its posttranslational modifications carried out in the secretory pathway. The mature AGP21 peptide contains only 10–13 aa in length. APO, apoplast; ER, endoplasmic reticulum; GPI anchor, glycosylphosphatidylinositol (GPI) anchor; PM, plasma membrane. (c) Co-localization of AGP21-Venus with BAK1-mRFP at the plasma membrane of epidermal cells in *Nicotiana benthamiana*. Bar, 10  $\mu$ m. Cross-section of expression levels across BAK1-RFP co-expressed with AGP21-Venus. On the left, plasmolysis was induced with 800 mM mannitol uncovering an apoplastic plus plasma membrane AGP21 localization. Arrowheads indicate plasma membrane located AGP21. Bar, 10  $\mu$ m. (d) Expression levels of AGP21-V (AGP21::V-AGP21/*agp21*) in atrichoblast (AT) and trichoblast (T) cell layers of the root meristematic zone. Bar, 10  $\mu$ m. (e) Immunoblot analysis of two stable lines expressing 35S::V-AGP21 (L1–L2) and two lines expressing AGP21::V-AGP21 (L1–L2) and two lines expressing AGP21::V-AGP21<sup>ALA</sup> (L1–L2). Each blot is an independent experiment. Putative Venus-AGP21 structures are indicated on the right based on the apparent molecular weight. O-Glycans are indicated as red elongated balloons.  $\Delta$ OH, non-hydroxylated;  $\Delta$ Gly, without O-glycans; 1-Gly to 3-Gly, 1 to 3 sites with Hyp-O-glycosylation. Asterisk indicates missing AGP21 glycoforms or lack of Venus protein. See also Supporting Information Figs S4–S6.

Individual residue RMSD analysis indicated that the peptide's stiffer region depended on the MD conditions applied (Fig. S6f). To characterize conformational profiles, we measured the angle formed by four consecutive alpha carbon atoms ( $\zeta$  angle) (Table S3). The  $\zeta$  angle of a type-II polyproline helix is –

$110^\circ \pm 15^\circ$ . In this context, the O-glycosylated AOAOSOTS peptide structure is slightly extended between Pro2–Thr7, as observed by  $\zeta$  angles 2–4 closer to  $180^\circ$  (Table S3). Our analysis suggests that O-linked glycans affect the conformation and stability of AGP21 peptide. How this conformational change in mature

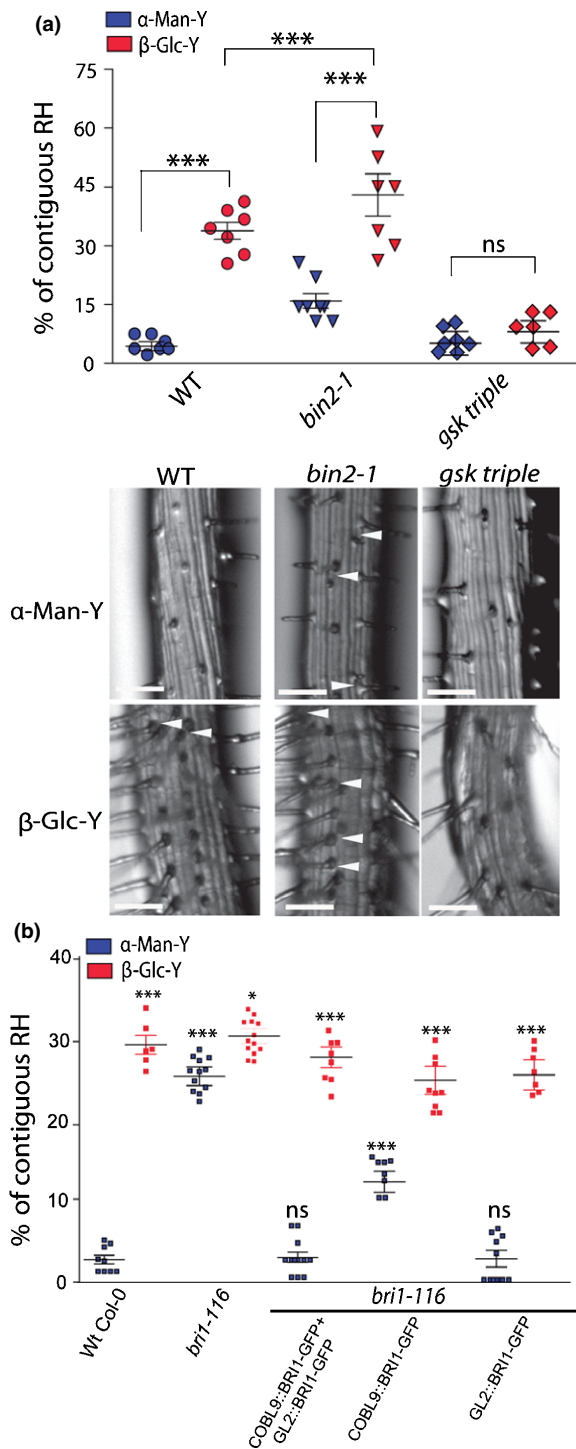


**Fig. 3** Perturbation of arabinogalactan proteins (AGPs) requires active BRI1 expression in atrichoblast cells and downstream BIN2-BIL1-BIL2 proteins to triggers changes in root hair (RH) cell fate in *Arabidopsis thaliana*. (a) Contiguous RH phenotype in roots treated with 5  $\mu$ M  $\beta$ -glucosyl Yariv ( $\beta$ -Glc-Y) or 5  $\mu$ M  $\alpha$ -mannosyl Yariv ( $\alpha$ -Man-Y). Bars, 20  $\mu$ m. *P*-value of one-way ANOVA: \*\*\*, *P* < 0.001; \*, *P* < 0.05; ns, not significant differences. Error bars indicate  $\pm$  SD from biological replicates. Arrowheads indicated two contiguous RHs. *bin2-1* is a constitutively active mutant of BIN2. *gsk triple* comprises *bin2-3 bil1 bil2* (BIN-2, BIL1 for BIN2-like 1 and BIL2 for BIN2-like 2). (b) Effect of the BRI1 differential expression on the development of contiguous RH. BRI1 is active when expressed in atrichoblast cells (under GL2 promoter). See also Supporting Information Fig. S5.

AGP21 peptide without *O*-glycans affects its function in RH cell determination remains unclear and merits further investigation in the future.

### AGP21 acts in a BIN2-dependent pathway to define RH cell fate

We hypothesized that disrupting AGPs activity with  $\beta$ -Glc-Y, a lack of AGP21 peptide (*agp21*), or abnormal glycosylation on AGP and related proteins, would interfere with BR responsiveness and RH cell fate. We treated the triple mutant *gsk* (*gsk triple: bin2-3 bil1 bil2*; BIL1, BIN2-like 1 and BIL2, BIN2-like 2), which almost completely lacks RH cells [1], with 5  $\mu$ M  $\beta$ -Glc-Y treatment. *Gsk triple* exhibited few contiguous RH cells before and after the treatment (Fig. 3), suggesting that  $\beta$ -Glc-Y requires BIN2-BIL1-BIL2 to alter RH cell fate. Interestingly,  $\beta$ -Glc-Y induced  $\approx$  40–45% contiguous RHs (Fig. 3) in the constitutively active mutant *bin2-1* (Li & Nam, 2002). These data suggest that the AGP-mediated RH cell fate reprogramming requires active BIN2, BIL1, and BIL2 proteins (Fig. 3a).

As *BRI1* expression is similar in trichoblast and atrichoblast cell layers (Fridman *et al.*, 2014), we sought to determine whether *BRI1* and downstream BR responses when AGPs are perturbed, act differently in these cell types during RH cell fate determination (Fig. 3b). We examined the effect of cell type-specific *BRI1* expression on the percentage of contiguous RHs in three plant lines expressing *BRI1*-GFP, all in the *bri1-116* background: trichoblast-only (*COBL9p::BRI1-GFP/bri1-116*), atrichoblast-only (*GL2p::BRI1-GFP/bri1-116*), and expression in both cell types (*GL2p::BRI1-GFP+ COBL9p::BRI1-GFP/bri1-116*) (Hacham *et al.*, 2011; Fridman *et al.*, 2014). *BRI1* expression in atrichoblasts did rescue *bri1-116* mutant RH phenotype as well as when *BRI1* was expressed in both cell types, being similar to wild-type (plants showed very low contiguous RHs). On the contrary, the line that expressed *BRI1* in trichoblasts showed higher contiguous RH than Wt Col-0 but lower than *bri1-116* (Fig. 3b). Additionally, *COBL9p::BRI1/bri1-116* where *BRI1* is expressed in trichoblast and missing in atrichoblast cells, it was still sensitive to  $\beta$ -Glc-Y. All the lines tested with *BRI1*-GFP exhibited high number of contiguous RHs with this treatment in similar trends than Wt Col-0 (Fig. 3b). These data imply that BR-*BRI1* pathway in atrichoblasts is highly sensitive to promote ectopic RH development under AGP disruption with  $\beta$ -Glc-Y and BR-*BRI1* in trichoblast also has an effect under  $\beta$ -Glc-Y. In addition, it is important to highlight *bri1-116* mutant high number of contiguous RHs is almost insensitive to  $\beta$ -Glc-Y treatment (Fig. 3b) suggesting that AGP-perturbation and its responses to trigger contiguous RH is mostly dependent on *BRI1*.

### Disturbance or absence of AGP21 blocks GL2 expression

We then tracked epidermal cell fate and analyzed the translational effects of  $\beta$ -Glc-Y and  $\alpha$ -Man-Y on several markers: an early RH marker (RHD6p::RHD6-GFP), a downstream transcription factor (RSL4p::RSL4-GFP), a late RH marker (EXP7p::EXP7-NLS-GFP), and two atrichoblast markers for GL2 (*GL2p::GFP* and



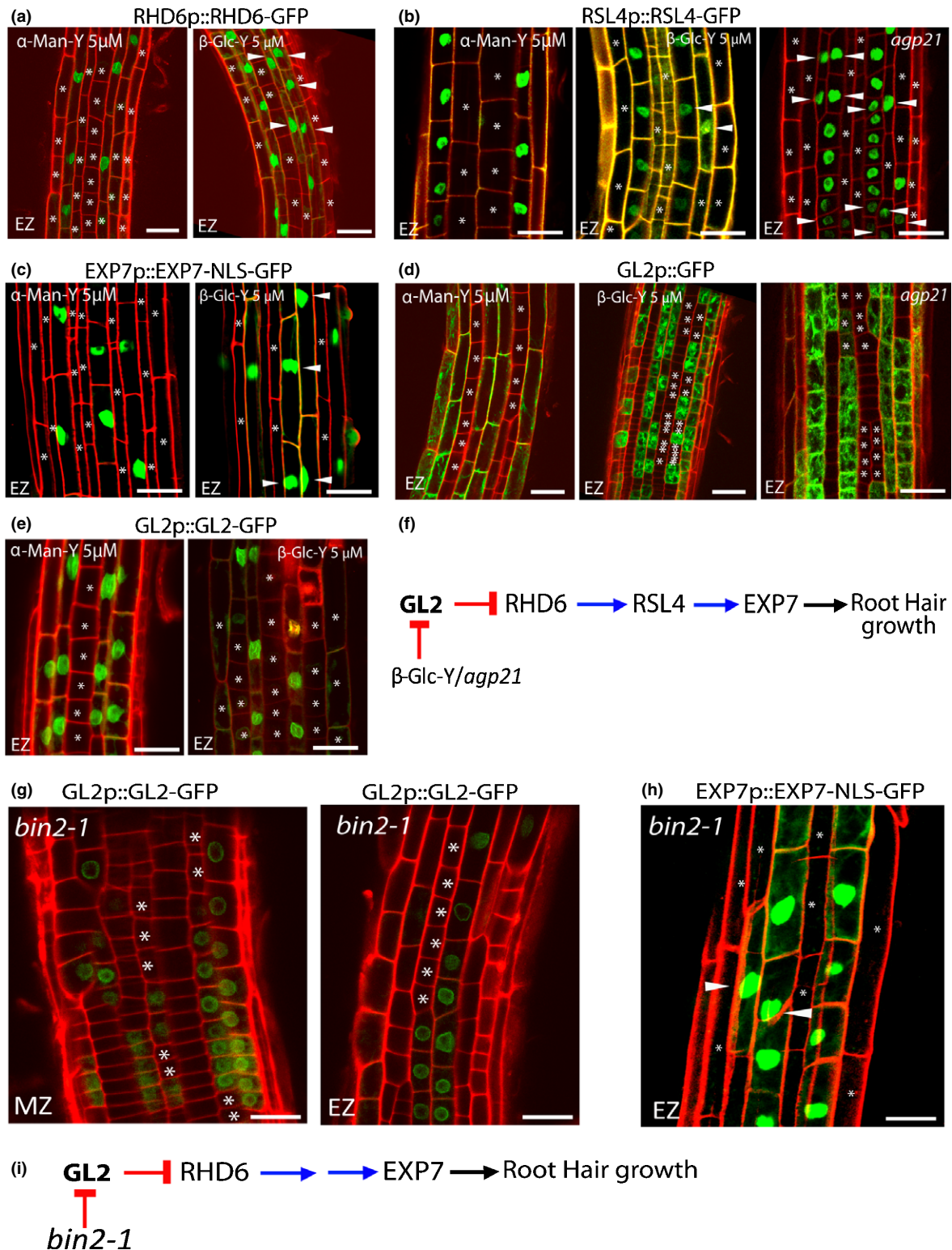


**Fig. 4** Arabinogalactan proteins (AGPs) disruption, the lack of AGP21, and *bin2-1* block the root hair (RH) repressor GLABRA2 (GL2) and triggers RHD6-RSL4-EXP7 expression in some atrichoblast cells in *Arabidopsis thaliana*. The effect of  $\beta$ -glucosyl Yariv ( $\beta$ -Glc-Y),  $\alpha$ -mannosyl Yariv ( $\alpha$ -Man-Y), and the absence of AGP21 peptide were monitored on several markers to study epidermis cell fate. (a) RHD6 (RHD6::RHD6-GFP) as an early RH marker. (b) A downstream RHD6 factor RSL4 (RSL4::RSL4-GFP). (c) The RSL4-gene target EXP7 (EXP7::EXP7-NLS-GFP). (d) The main RH repressor GL2 as a transcriptional marker (GL2::GFP). (e) The main RH repressor GL2 as a translational marker (GL2::GL2-GFP). (f) Proposed sequence of events triggered by  $\beta$ -Glc-Y or the lack of AGP21 peptide that leads to abnormal RH development. (g) GL2 expression (GL2::GL2-GFP) in the *bin2-1* background in the meristematic zone (MZ) and elongation zone (EZ) of the root. (h) The RH marker EXP7 expression (EXP7::EXP7-NLS-GFP) in the *bin2-1* background in the EZ of the root. (a–e and g–h) Arrowheads indicate expression of a given marker in two contiguous epidermal cell lines. Asterisks indicated absence of expression. Bars, 20  $\mu$ m. (i) Proposed sequence of events triggered by *bin2-1* that leads to abnormal RH development. See also Supporting Information Fig. S7.

GL2p::GL2-GFP) (Fig. 4a–e).  $\beta$ -Glc-Y, not  $\alpha$ -Man-Y, repressed GL2 expression and enhanced RHD6, RSL4 and EXP7 expression in contiguous epidermal cells (Fig. 4a–e). This corroborates the effects of both  $\beta$ -Glc-Y and deficiencies in the AGP *O*-glycosylation pathway on contiguous epidermal cell development. Then, when we expressed RSL4p::RSL4-GFP in *agp21*, two contiguous epidermal cells showed GFP expression, while this rarely occurred in wild-type roots (Fig. 4b). The transcriptional reporter GL2p::GFP/*agp21* showed discontinuous RH patterning similar to  $\beta$ -Glc-Y treatment (Fig. 4d). This result implies feedback between the lack of AGP21, GL2 repression, and RHD6-RSL4 and EXP7 positive regulation in contiguous epidermal cell development (Fig. 4f). Constitutively active *bin2-1* phenocopies *agp21* and  $\beta$ -Glc-Y treatment: it represses GL2 expression in some epidermal cells and enhances EXP7-GFP in contiguous epidermal cells, stimulating contiguous RH development (Fig. 4g,h). In addition, the overall levels of GL2 expression are much lower in *bin2-1* than in Col-0. To test whether AGP21 (and AGPs in general), affect BR responses, we treated roots with 100 nM BL. Wild-type roots exhibited repressed RH development as previously reported (Cheng *et al.*, 2014); *agp21* and three GT mutants (*triple hpgt*, *ray1* and *galt29A*) defective in AGP *O*-glycosylation (Table S1) were unaffected by BL treatment (Fig. S5c), suggesting that *O*-glycosylated AGP21 (and AGPs) are required for promoting BR responses and downstream signaling on RH cell fate.

## Conclusions

In root epidermal cells, atrichoblast fate is the default, while environmental as well as endogenous cues like high levels of BRs promotes *GL2* expression in atrichoblasts to repress RH development (Cheng *et al.*, 2014). In the absence of BRs, active P-BIN2 represses *GL2* expression and *RHD6* and *RSL4* expression proceeds, triggering RH development in atrichoblasts and producing contiguous RHs. Perturbed AGPs and the lack of AGP21 peptide at the cell surface stimulate ectopic RH development (in atrichoblast cells that developed as trichoblasts) similar to that observed in BR mutants. BZR1 regulates *AGP21* expression and the *O*-glycosylated cell surface peptide AGP21 modulates RH cell fate. We propose a model, in which the *O*-glycosylated AGP21 peptide and BR responses are both dependent on BIN2 (and BIL1-BIL2)-mediated responses, controlling RH cell fate (Fig. S7). It is still unclear how the cell surface peptide AGP21 is able to trigger a change in RH cell fate in a BIN2-dependent manner. One possibility is that AGP21 peptide might modify the responsiveness to BRs of the co-receptors BRI1-BAK1. In line with this, we failed to detect a direct interaction between V-AGP21 and BAK1-mRFP in a transient expression system (results not shown). Nonetheless, measuring direct physical interactions between *O*-glycosylated AGP21 and BRI1-BAK1 proteins in the apoplast-PM space is a challenge for a future study. In concordance with this scenario, other GPI anchor proteins (e.g. like LORELEI-like-GPI-anchored protein 2 and 3, LRE/LLG2,3) are able to interact with CrRLK1s (e.g. FERONIA and BUP1,2/ANXUR1,2) in the cell surface of polar growing plant cells (Feng *et al.*, 2019; Ge *et al.*, 2019; Li *et al.*,

2015, 2016; Liu *et al.*, 2016). These results imply an interesting parallel between plant AGPs and animal heparin sulfate proteoglycans (HSPGs), which are important co-receptors in signaling pathways mediated by growth factors, including members of Wnt/Wingless, Hedgehog, transforming growth factor- $\beta$ , and fibroblast growth factor family members (Lin, 2004). A second scenario is that AGP21 peptide and BR co-receptors BRI1-BAK1 do not interact in the cell surface and both influence by different pathways BIN2 activity and the downstream RH cell fate program. If this is the case, AGP21 may require other proteins to transduce the signal toward BIN2 in the cytoplasm. Future work should investigate which of these two hypotheses might explain the role of AGP21 peptide in RH cell fate.

## Acknowledgements

The authors thank ABRC (Ohio State University) for providing T-DNA lines seed lines. The authors would like to thank Dr Sigal Savaldi-Goldstein for providing GL2::BRI1-GFP, COBL9::BRI1-GFP and GL2::BRI1-GFP+COBL9::BRI1-GFP reporter lines, Dr Paul Dupree for providing *fut4* and *fut6* mutant lines, Dr Santiago Mora García for providing *bzr1* and *bes1* mutant lines, Dr Ana Caño Delgado for providing seeds of BRI1-GFP, *bin2-1* and BZR-YFP, and Dr Gustavo Gudesblat for providing *gsk* triple mutant seeds. Dr Malcolm Bennet and Dr Liam Dolan for the RHD6-GFP and RSL4-GFP lines. This work was supported by grants from ANPCyT (PICT2014-0504, PICT2016-0132 and PICT2017-0066), ICGEB CRP/ARG16-03, and Instituto Milenio iBio – Iniciativa Científica Milenio, MINECON to JME.

## Author contributions

CB, JGD and MMR performed most of the experiments, analyzed the data and wrote the paper. MCS analyzed the phenotype of glycosyltransferase mutants and BRI1-GFP reporters. LPF and HV performed molecular dynamics simulations and analyzed this data. BV analyzed the molecular dynamics simulations data. MC synthesized  $\alpha$ -Man-Y and  $\beta$ -Glc-Y reagents. GS commented on the project, read the manuscript, and commented on the results. SM and EM analyzed the data and commented on the results. JMP, DRRG, YdCRG and SMV commented on the results. JME designed research, supervised the project, and wrote the paper. CB, JGD and MMR contributed equally to this work. This manuscript has not been published and is not under consideration for publication elsewhere. All the authors have read the manuscript and have approved this submission.

## ORCID

José M. Estevez  <https://orcid.org/0000-0001-6332-7738>

## References

- Balcerowicz D, Schoenaers S, Vissenberg K. 2015. Cell fate determination and the switch from diffuse growth to planar polarity in Arabidopsis root epidermal cells. *Frontiers in Plant Science* 6: 949.

- Barnett NM. 1970. Dipyrindyl-induced cell elongation and inhibition of cell wall hydroxyproline biosynthesis. *Plant Physiology* 45: 188–191.
- Berendsen HJC, Grigera JR, Straatsma TPJ. 1987. The missing term in effective pair potentials. *The Journal of Physical Chemistry* 91: 6269–6271.
- Berendsen HJC, Postma JPM, van Gunsteren WF, DiNola A, Haak JR. 1984. Molecular-dynamics with coupling to an external bath. *The Journal of Chemical Physics* 81: 3684–3690.
- Bussi G, Donadio D, Parrinello MJ. 2007. Canonical sampling through velocity rescaling. *The Journal of Chemical Physics* 126: 014101.
- Cheng Y, Zhu W, Chen Y, Ito S, Asami T, Wang X. 2014. Brassinosteroids control root epidermal cell fate via direct regulation of a MYBBHLH-WD40 complex by GSK3-like kinases. *eLife* 3: e02525.
- Ding L, Zhu JK. 1997. A role for arabinogalactan-proteins in root epidermal cell expansion. *Planta* 203: 289–94.
- Feng H, Liu C, Fu R, Zhang M, Li H, Shen L, Wei Q, Sun X, Xu L, Ni B *et al.* 2019. LORELEI-LIKE GPI-ANCHORED PROTEINS 2/3 regulate pollen tube growth as chaperones and coreceptors for ANXUR/BUPS receptor kinases in Arabidopsis. *Molecular Plant* 12: 1612–1623.
- Fridman Y, Elkouby L, Holland N, Vragovic K, Elbaum R, Savaldi-Goldstein S. 2014. Root growth is modulated by differential hormonal sensitivity in neighboring cells. *Genes & Development* 28: 912–920.
- Ge Z, Zhao Y, Liu M-Ch, Zhou L-Z, Wang L, Zhong S, Hou S, Jiang J, Liu T, Huang Q *et al.* 2019. LLG2/3 are co-receptors in BUPS/ANX-RALF signaling to regulate Arabidopsis pollen tube integrity. *Current Biology* 29: 1–10.
- Guan Y, Nothnagel EA. 2004. Binding of arabinogalactan proteins by Yariv phenylglycoside triggers wound-like responses in Arabidopsis cell cultures. *Plant Physiology* 135: 1346–136.
- Hacham Y, Holland N, Butterfield C, Ubeda-Tomas S, Bennett MJ, Chory J, Savaldi-Goldstein S. 2011. Brassinosteroid perception in the epidermis controls root meristem size. *Development* 138: 839–848.
- Hess B, Bekker H, Berendsen HJC, Fraaije JGEM. 1997. LINCOS: A linear constraint solver for molecular simulations. *Journal of Computational Chemistry* 18: 1463–1472.
- Hess B, Kutzner C, Van Der Spoel D, Lindahl E. 2008. GROMACS 4: Algorithms for highly efficient, load-balanced, and scalable molecular simulation. *Journal of Chemical Theory and Computation* 4: 435–444.
- Hothorn M, Belkhadir Y, Dreux M, Dabi T, Noel JP, Wilson IA, Chory J. 2011. Structural basis of steroid hormone perception by the receptor kinase BRI1. *Nature* 474: 467–471.
- Kitazawa K, Tryfona T, Yoshimi Y, Hayashi Y, Kawauchi S, Antonov L, Tanaka H, Takahashi T, Kaneko S, Dupree P *et al.* 2013.  $\beta$ -Galactosyl Yariv reagent binds to the  $\beta$ -1,3-galactan of arabinogalactan proteins. *Plant Physiology* 161: 1117–1126.
- Kuppusamy KT, Chen AY, Nemhauser JL. 2009. Steroids are required for epidermal cell fate establishment in Arabidopsis roots. *Proceedings of the National Academy of Sciences, USA* 106: 8073–8076.
- Li C, Wu H-M, Cheung AY. 2016. FERONIA and her pals: functions and mechanisms. *Plant Physiology* 171: 2379–2392.
- Li C, Yeh FL, Cheung AY, Duan Q, Kita D, Liu MC, Maman J, Luu EJ, Wu BW, Gates L *et al.* 2015. Glycosylphosphatidylinositol anchored proteins as chaperones and co-receptors for FERONIA receptor kinase signaling in Arabidopsis. *eLife* 4: e06587.
- Li J, Chory J. 1997. A putative leucine-rich repeat receptor kinase involved in brassinosteroid signal transduction. *Cell* 90: 929–938.
- Li J, Nam KH. 2002. Regulation of brassinosteroid signaling by a GSK3/SHAGGY-like kinase. *Science* 295: 1299–1301.
- Liang Y, Basu D, Pattathil S, Xu W-L, Venetos A, Martin SL, Faik A, Hahn MG, Showalter AM. 2013. Biochemical and physiological characterization of fut4 and fut6 mutants defective in arabinogalactan-protein fucosylation in Arabidopsis. *Journal of Experimental Botany* 64: 5537–5551.
- Lin Q, Ohashi Y, Kato M, Tsuge T, Gu H, Qu LJ, Aoyama T. 2015. GLABRA2 directly suppresses basic helix-loop-helix transcription factor genes with diverse functions in root hair development. *Plant Cell* 27: 2894–2906.
- Lin X. 2004. Functions of heparan sulfate proteoglycans in cell signaling during development. *Development* 131: 6009–6021.
- Liu X, Castro C, Wang Y, Noble J, Ponvert N, Bundy M, Hoel C, Shpak E, Palanivelu R. 2016. The role of LORELEI in pollen tube reception at the interface of the synergid cell and pollen tube requires the modified eight-cysteine motif and the receptor-like kinase FERONIA. *Plant Cell* 28: 1035–1052.
- Ma Y, Zeng W, Bacic A, Johnson K. 2018. AGPs through time and space. *Annual Plant Reviews* 1: 1–38.
- Majamaa K, Gunzler V, Hanauske-Abel HM, Myllylä R, Kivirikko KI. 1986. Partial identity of the 2-oxoglutarate and ascorbate binding sites of prolyl 4-hydroxylase. *Journal of Biological Chemistry* 261: 7819–7823.
- Masucci JD, Schiefelbein JW. 1994. The rhd6 mutation of Arabidopsis thaliana alters root-hair initiation through an auxin- and ethylene-associated process. *Plant Physiology* 106: 1335–1346.
- Masucci JD, Schiefelbein JW. 1996. Hormones act downstream of TTG and GL2 to promote root hair outgrowth during epidermis development in the Arabidopsis root. *The Plant Cell* 8: 1505–1517.
- Motose H, Sugiyama M, Fukuda H. 2004. A proteoglycan mediates inductive interaction during plant vascular development. *Nature* 429: 873–878.
- Ogawa-Ohnishi M, Matsubayashi Y. 2015. Identification of three potent hydroxyproline O-galactosyltransferases in Arabidopsis. *The Plant Journal* 81: 736–746.
- Pereira AM, Pereira LG, Coimbra S. 2015. Arabinogalactan proteins: rising attention from plant biologists. *Plant Reproduction* 28: 1–15.
- Pol-Fachin L, Verli H. 2012. Structural glycochemistry of the major allergen of Artemisia vulgaris pollen, Art v 1: O-glycosylation influence on the protein dynamics and allergenicity. *Glycobiology* 22: 817–825.
- Ryu KH, Kang YH, Park YH, Hwang I, Schiefelbein J, Lee MM. 2005. The WEREWOLF MYB protein directly regulates CAPRICE transcription during cell fate specification in the Arabidopsis root epidermis. *Development (Cambridge, England)* 132: 4765–4775.
- Sardar HS, Yang J, Showalter AM. 2006. Molecular interactions of arabinogalactan proteins with cortical microtubules and F-actin in Bright Yellow-2 tobacco cultured cells. *Plant Physiology* 142: 1469–1479.
- Savaldi-Goldstein S, Peto C, Chory J. 2007. The epidermis both drives and restricts plant shoot growth. *Nature* 446: 199–202.
- Schiefelbein J, Huang L, Zheng X. 2014. Regulation of epidermal cell fate in Arabidopsis roots: the importance of multiple feedback loops. *Frontiers in Plant Science* 5: 47.
- Schultz CJ, Ferguson KL, Lahnstein J, Bacic A. 2004. Post-translational modifications of arabinogalactan-peptides of Arabidopsis thaliana: endoplasmic reticulum and glycosylphosphatidylinositol-anchor signal cleavage sites and hydroxylation of proline. *Journal of Biological Chemistry* 279: 45503–45511.
- Seifert GJ, Roberts K. 2007. The biology of arabinogalactan proteins. *Annual Review of Plant Biology* 58: 137–161.
- She J, Han Z, Kim TW, Wang J, Cheng W, Chang J, Shi S, Wang J, Yang M, Wang ZY *et al.* 2011. Structural insight into brassinosteroid perception by BRI1. *Nature* 474: 472–476.
- Song SK, Ryu KH, Kang YH, Song JH, Cho YH, Yoo SD, Schiefelbein J, Lee MM. 2011. Cell fate in the Arabidopsis root epidermis is determined by competition between WEREWOLF and CAPRICE. *Plant Physiology* 157: 1196–1208.
- Sun Y, Fan XY, Cao DM, Tang W, He K, Zhu JY, He JX, Bai MY, Zhu S, Oh E *et al.* 2010. Integration of brassinosteroid signal transduction with the transcription network for plant growth regulation in Arabidopsis. *Developmental Cell* 19: 765–777.
- Tan L, Qiu F, Lampion DTA, Kieliszewski MJ. 2004. Structure of a hydroxyproline (Hyp)-arabinogalactan polysaccharide from repetitive Ala-Hyp expressed in transgenic Nicotiana tabacum. *Journal of Biological Chemistry* 279: 13156–13165.
- Tironi IG, Sperber R, Smith PE, van Gunsteren WF. 1995. A generalized reaction field method for molecular-dynamics simulations. *The Journal of Chemical Physics* 102: 5451–5459.
- Tryfona T, Theys TE, Wagner T, Stott K, Keegstra K, Dupree P. 2014. Characterisation of FUT4 and FUT6  $\alpha$ -(1→2)-fucosyltransferases reveals that absence of root arabinogalactan fucosylation increases Arabidopsis root growth salt sensitivity. *PLoS ONE* 9: e93291.
- Van Hengel AJ, Barber C, Roberts K. 2004. The expression patterns of arabinogalactan-protein AtAGP30 and GLABRA2 reveal a role for abscisic acid in the early stages of root epidermal patterning. *The Plant Journal: for Cell and Molecular Biology* 39: 70–83.
- Velasquez SM, Marzol E, Borassi C, Pol-Fachin L, Ricardi MM, Mangano S, Denita Juarez SP, Salgado Salter JD, Gloazzo Dorosz J, Marcus SE *et al.* 2015b.

- Low sugar is not always good: impact of specific *O*-glycan defects on tip growth in *Arabidopsis*. *Plant Physiology* 168: 808–813.
- Velasquez SM, Ricardi MM, Dorosz JG, Fernandez PV, Nadra AD, Pol-Fachin L, Egelund J, Gille S, Ciancia M, Verli H *et al.* 2011. *O*-Glycosylated cell wall extensins are essential in root hair growth. *Science* 332: 1401–1403.
- Velasquez SM, Ricardi MM, Poulsen CP, Oikawa A, Dilokpimol A, Halim A, Mangano S, Denita Juarez SP, Marzol E, Salgado Salter JD *et al.* 2015a. Complex regulation of prolyl-4-hydroxylases impacts root hair expansion. *Molecular Plant* 8: 734–746.
- Willats WG, Knox JP. 1996. A role for arabinogalactan-proteins in plant cell expansion: evidence from studies on the interaction of  $\beta$ -glucosyl Yariv reagent with seedlings of *Arabidopsis thaliana*. *The Plant Journal* 9: 919–25.
- Xu J, Tan L, Lampert DTA, Showalter AM, Kieliszewski MJ. 2008. The *O*-Hyp glycosylation code in tobacco and *Arabidopsis* and a proposed role of Hyp-glycans in secretion. *Phytochemistry* 69: 1631–1640.
- Xue H, Veit C, Abas L, Tryfona T, Maresch D, Ricardi MM, Estevez JM, Strasser R, Seifert GJ. 2017. *Arabidopsis thaliana* FLA4 functions as a glycan-stabilized soluble factor via its carboxy proximal Fasciclin 1 domain. *The Plant Journal* 91: 613–630.
- Yan Z, Zhao J, Peng P, Chihara RK, Li J. 2009. BIN2 functions redundantly with other *Arabidopsis* GSK3-like kinases to regulate brassinosteroid signaling. *Plant Physiology* 150: 710–721.
- Yang CJ, Zhang C, Lu YN, Jin JQ, Wang XL. 2011. The mechanisms of brassinosteroids' action: from signal transduction to plant development. *Molecular Plant* 4: 588–600.
- Yariv J, Lis H, Katchalski E. 1967. Precipitation of arabic acid and some seed polysaccharides by glycosylphenylazo dyes. *The Biochemical Journal* 105: 1C–2C.
- Yi K, Menand B, Bell E, Dolan L. 2010. A basic helix-loop-helix transcription factor controls cell growth and size in root hairs. *Nature Genetics* 42: 264–267.

## Supporting Information

Additional Supporting Information may be found online in the Supporting Information section at the end of the article.

**Fig. S1** Perturbation of *O*-glycosylated AGPs affect RH cell fate program.

**Fig. S2** Expression pattern of enzymes involved in proline hydroxylation and *O*-glycosylation of AGPs in the *Arabidopsis* epidermis root.

**Fig. S3** BR deficiency triggers RH abnormal development and BR control of AGP21 expression.

**Fig. S4** Characterization of *agp21* and *agp15* mutants.

**Fig. S5** AGP21 expression at the cell surface in epidermis and RH cells.

**Fig. S6** *O*-Glycans provide stability to the AGP21 peptide conformation.

**Fig. S7** AGP21 peptide influences RH cell fate in a BIN2-dependent manner.

**Table S1** Primers used in this study.

**Table S2** Mutants and transgenic lines generated and used in this study.

**Table S3** Average  $\zeta$  angle values\* during the performed MD simulations of AGP21 peptide.

**Table S4** GTs involved in AGP modification used in this study.

Please note: Wiley Blackwell are not responsible for the content or functionality of any Supporting Information supplied by the authors. Any queries (other than missing material) should be directed to the *New Phytologist* Central Office.